

Production and thermal annealing of neutrino-recoil-induced Frenkel pairs in copper

H. Metzner, R. Sielemann, S. Klaumünzer, and E. Hunger

Hahn-Meitner-Institut, Bereich Kern-und Strahlenphysik, D-1000 Berlin 39, Germany

and Freie Universität Berlin, Fachbereich Physik, D-1000 Berlin 33, Germany

(Received 27 May 1987)

^{111}In atoms which originate from ^{111}Sn decays via electron capture start at the energy of 29 eV from substitutional lattice sites in otherwise undamaged copper and produce isolated single Frenkel pairs at 4.2 K. The observation of $\gamma\gamma$ perturbed angular correlations (PAC's) following the decay of ^{111}In to ^{111}Cd yields the signal of the copper monovacancy of $\nu_Q = e^2 Qq/h = 117$ MHz ($\eta=0$). The thermal annealing behavior of the Frenkel pairs is studied by PAC in an isochronal (10-min) annealing program between 4.2 and 300 K. Two distinct annealing steps are observed: Between 35 and 48 K about 60% and between 250 and 293 K the remaining 40% of the monovacancies vanish. The first step is due to the recombination of vacancies with their own interstitial (correlated recombination), while the second one is caused by detrapping and free vacancy migration. Details of the process of Frenkel-pair production and consequences for defect models are discussed.

I. INTRODUCTION

The production of single Frenkel pairs is the elementary process of defect production in metals by particle irradiation. Therefore, considerable theoretical and experimental effort has been devoted to this process and to related phenomena like thermally activated Frenkel-pair (FP) annealing.¹ The most-detailed studies were performed for copper which thus became kind of a model substance in this research field. Experimentally, single FP's can be produced by electron irradiation, and the number of FP's can easily be monitored by resistivity measurements. Experiments of such type were used to determine the threshold energy surface for FP production in copper^{2,3} and thoroughly to investigate the characteristic resistivity stages that are observed as a consequence of different annealing processes.⁴

However, microscopic information on FP production stems from computer simulations only, which were performed with atomic potentials representing copper.^{5,6} These simulations suggest two basic features of the production process: mass transport by replacement collisions combined with an efficient energy transport along close-packed lattice directions due to focusing effects. A direct experimental verification of these findings is, however, still outstanding.

Microscopic experimental information is available from nuclear probe methods like $\gamma\gamma$ perturbed angular correlations (PAC's) and Mössbauer spectroscopy (MS). Both these methods have, in the last decade, considerably contributed to the understanding of phenomena related to point defects in metals.⁷ The main advantage of PAC's (and MS) is the unique possibility to distinguish and recognize defects by their characteristic hyperfine interaction with nuclear probes. However, a defect is usually detectable only if a trapping process occurs during the course of thermally activated defect migration. Therefore, PAC's (and MS) could hitherto not be used to

investigate FP production and correlated FP recombination, since information on both these processes is lost when free defect migration occurs.

We have shown that this experimental limitation can be circumvented if the ^{111}In - ^{111}Cd PAC probe is not used as a trap but rather as a primary knock-on atom (PKA) in single-FP production.⁸ In this experiment the monoenergetic knock-on atom is provided by neutrino recoil in the β decay of ^{111}Sn to ^{111}In via orbital electron capture.⁹ We have repeated the experiment with considerable improvements that allow us to perform a fairly detailed annealing program and to accumulate PAC spectra with higher accuracy. Thus we are now able to follow up the production and annealing of single FP's in copper from the microscopic viewpoint of the nuclear ^{111}In - ^{111}Cd probe.

In the following section we describe FP production by neutrino recoil, the experimental realization of this effect, and experimental details. The experimental results, their implications for the understanding of FP production and annealing, and a comparison to existing defect models are discussed in Sec. III.

II. EXPERIMENT

A. Frenkel-pair production by neutrino recoil

If a lattice atom in a metal is knocked from its lattice site with an energy exceeding the threshold E_d , it will produce a single FP. Above $2E_d$ multiple-defect production becomes possible. It is well known that E_d has not one fixed value (for one metal), but is rather a function of lattice direction $\langle hkl \rangle$. In copper, E_d has a minimum of $E_{d,\text{min}} = 19$ eV and E_d ranges from 19 to 23 eV for PKA momenta along or close to the $\langle 110 \rangle$ and $\langle 100 \rangle$ directions.¹ Very high values of $E_d > 50$ eV are found, e.g., in or close to $\langle 111 \rangle$ directions.¹ The low values of E_d along $\langle 110 \rangle$ and $\langle 100 \rangle$ are explained by

replacement collision sequences accompanied by Silsbee focusing¹⁰ or assisted focusing,⁵ respectively. The focusing effects ensure a rather efficient energy transport and the straight propagation of the collision sequence. As a result of such a replacement collision sequence a certain number of atoms including the PKA will occupy former neighboring sites along one atomic chain. The former site of the PKA is left as a vacancy.¹¹ The last replaced atom will be part of an interstitial configuration. One FP is thus produced. It will be stable (at $T=0$) only if the interstitial is formed at least a certain minimum distance away from the vacancy.

The current knowledge about FP production outlined above refers to pure copper, while in our experiment isolated ¹¹¹In atoms are used as PKA's. This implies some peculiarities which we discuss below.

¹¹¹Sn (half-life $T_{1/2}=35$ min) decays to the ground state of ¹¹¹In via electron capture (EC) in 61% of all cases.¹² In this β decay a ¹¹¹Sn K electron (binding energy $E_b=29$ keV) is captured into the nucleus and a neutrino is emitted.¹³ Because of momentum conservation the neutrino carries away virtually the whole decay energy Q_{EC} of the EC decay. The recoil energy E_r of the resulting ¹¹¹In ion is only very small:

$$E_r = (Q_{EC} - E_b)^2 / 2Mc^2 = 29 \text{ eV} . \quad (1)$$

$Q_{EC}/c^2 = 2465 \pm 12 \text{ keV}/c^2$ is the mass difference between the neutral ¹¹¹Sn and ¹¹¹In atoms¹⁴ and M is the ¹¹¹In mass. The maximum energy E_{max} a 29-eV ¹¹¹In recoil atom can transfer to its copper neighbor in an elastic collision is given by

$$E_{max} = E_r 4m_{Cu}m_{In} / (m_{Cu} + m_{In})^2 = 27 \text{ eV} . \quad (2)$$

This energy lies well in the interesting energy window between $E_{d,min}$ and $2E_{d,min}$, i.e., between 19 and 38 eV, so that exclusively single FP's are produced. The decay channels of the remaining 39% of ¹¹¹Sn atoms lead to ¹¹¹In recoil energies of maximum 17 eV,⁸ so that this fraction does not contribute to FP production.

Thus all produced FP's can definitely be assigned to the PKA energy of 29 eV. This is an advantage compared to electron irradiation which is usually employed for single-FP production. In these experiments it is difficult to relate a certain type of FP (or a resulting annealing stage) to a certain PKA energy,¹⁵ since all recoil energies of a PKA up to a certain limit occur. Moreover, for exclusive single-Frenkel-pair production a low electron energy for which the maximum PKA energy lies below $2E_{d,min}$ has to be chosen. For such low electron energies, however, the cross section for energy transfers above $E_{d,min}$, i.e., for FP production, is very low.¹⁶ This is one reason why most electron-irradiation experiments were performed with much higher electron energies. For example, Corbett, Smith, and Walker used 1.4-MeV electrons corresponding to a maximum PKA energy of 115 eV.⁴

The price of this unique possibility to study the fate of the PKA microscopically is the use of the ¹¹¹In impurity. Thus, we have to keep in mind the impurity character of the ¹¹¹In PKA when comparing both FP production and annealing to the case of pure copper, since both

phenomena could be modified by the impurity.

As far as the production process is concerned, we are in an energy regime in which only the repulsive part of a (hypothetical) two-body potential is important, so that a two-body-collision model might apply.¹⁰ If this is the case, already very simple calculations should yield some insight into the problem. We performed such calculations in the hard-sphere approximation (see Appendix). The hard-sphere radius of a copper atom was taken as half the distance of closest approach (at 30 eV) for a pair potential given by Gibson *et al.*⁵ Since a reliable two-body potential for In in Cu is not available, the hard-sphere radius of the In atom was then assumed to be 21% larger, i.e., the same amount as the atomic radius increases if a Cu atom is replaced by an In atom in a Cu matrix.¹⁷ The mass difference was considered as indicated by Eq. (2). Within this model we considered the Silsbee case (collisions along $\langle 110 \rangle$) and find better focusing characteristics due to the oversized In PKA (see Appendix). However, in the present case these will be compensated by the reduced energy transfer so that altogether $\langle 110 \rangle$ collision chains initiated by the In PKA should be very similar to those in pure copper. The large hard-sphere radius of In will, however, be important for collisions along $\langle 100 \rangle$, since the In atom has to pass a window of four nearest-neighbor copper atoms in order to hit its next-nearest $\langle 100 \rangle$ neighbor. This effect might lead to an increased threshold along $\langle 100 \rangle$ (see also Sec. III B).

The effect of the In impurity on FP annealing is not *a priori* clear, especially if we are dealing with close FP's. Both Frenkel partners and the oversized impurity In induce lattice distortions which can altogether lead to anisotropic attractive and repulsive forces between any pair of the three constituents. It is known from experiment that there is a high probability for correlated FP recombination in pure copper,⁴ and that In impurities can trap interstitials as well as vacancies in copper.⁷

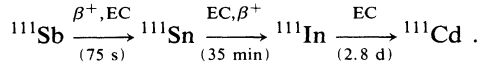
B. Experimental realization

The short half-life of ¹¹¹Sn of 35 min requires a quasi-online production of the probe activity. The experiments were performed using the heavy-ion accelerator facility VICKSI at the Hahn-Meitner-Institute in Berlin. Heavy-ion-induced reactions not only allow a rather selective production of a desired probe nucleus, but also produce these nuclei at high recoil energies well suited for recoil implantation techniques.

We used reactions induced by ²²Ne on ⁹³Nb, because ²²Ne (up to 100 MeV) is a high-intensity beam of VICKSI and niobium has only one stable isotope. Using the nuclear-physics computer code CASCADE,¹⁸ we obtained 90 MeV as the optimum beam energy. Three relevant reaction channels lead to nuclei with mass $A=111$ at this beam energy. The respective reaction cross sections $\sigma_{a,b,c}$ were also calculated by means of CASCADE:

- (a) ⁹³Nb(²²Ne,4n)¹¹¹Sb, $\sigma_a = 83$ mb.
- (b) ⁹³Nb(²²Ne,p3n)¹¹¹Sn, $\sigma_b = 204$ mb.
- (c) ⁹³Nb(²²Ne,2p2n or α)¹¹¹In, $\sigma_c = 32$ mb.

The β -decay chain for $A = 111$ (Ref. 19) is given for comparison (half-lives in parentheses):



The experimental time table is essentially governed by the ^{111}Sn half-life. A reasonable fraction of the probe atoms was obtained as ^{111}Sn by choosing an irradiation time of $t_1 = (30 \pm 1)$ min. The half-life of ^{111}Sb can then be neglected and both reactions (a) and (b) lead to the desired ^{111}Sn nuclei. In reaction (c) ^{111}In is produced directly. These ^{111}In atoms therefore only contribute to the PAC measurement but not to the neutrino recoil effect. This is taken into account by an experimental reduction factor which is defined by Eq. (3) (see below).

The experiment is performed as follows: A copper foil of 99.999% nominal purity obtained from Materials Research Company is rolled to $2 \mu\text{m}$ thickness and well annealed. This foil is covered with a $2\text{-}\mu\text{m}$ -thin niobium foil and fixed in a target holder. This target is bombarded with ^{22}Ne ions of 90 MeV so that the nuclear reactions discussed above are induced in the niobium foil. The product nuclei receive kinetic energies up to 18 MeV. Therefore the product nuclei leave the niobium foil and are stopped in the copper foil. Undesired radioactivity produced in the copper foil as well as ^{22}Ne ions that do not suffer any nuclear reaction are stopped in a thick gold-plated copper backing which is water cooled. The target area is 0.8 cm^2 , and we use the maximum beam current of VICKSI for the ^{22}Ne beam of about 3×10^{12} ions/s. After the irradiation the copper foil is annealed in a tube furnace at 550°C for 2 min in streaming gas containing 95 mol % Ar and 5 mol % H_2 . This procedure ensures that all defects created during heavy-ion bombardment (and by preceding β decays) are annealed. As a result, all probes are located on undisturbed substitutional cubic sites as proven in a PAC check experiment described previously.⁸ After the anneal the copper sample is taped to a small Plexiglass vessel which is then lowered into a liquid-helium (LHe) bath and fixed in a well-defined position. At 4.2 K all point defects in copper are immobile.⁴ The point of time at which the sample enters the helium bath is the time zero for observable FP production. The time t_2 needed from the end of irradiation to this time zero is $t_2 = (9 \pm 1)$ min.

We performed two measuring runs for each of which 10 copper samples were doped with ^{111}Sn as described. This allowed the performance of a PAC-controlled annealing program in which each PAC spectrum is of good statistical accuracy. In each annealing step the ten samples were simultaneously drawn up into the He-gas column until the desired temperature was reached. The temperature was measured by a calibrated carbon resistor and two calibrated Fe-Constantan thermocouples which were fixed above and below the resistor in order to monitor the temperature gradient along the sample height of 1 cm. Though the temperature could be kept fairly constant throughout the annealing time of 10 min, a maximum error of ± 2 K for all annealing temperatures has to be conceded because of the mentioned tem-

perature gradient. For the sake of simplicity the PAC spectra of the annealing points above 100 K were measured at 77 K using a liquid-nitrogen bath, and the anneals were performed in the N_2 column.

For the correct scaling of the neutrino-recoil effect we have to calculate the fraction f_n of probes which are capable of producing FP's after the above-mentioned "time zero" of FP production. This fraction is calculated as follows:

$$f_n = \frac{\sigma_a + \sigma_b}{\sigma_a + \sigma_b + \sigma_c} f_{\text{EC}} \frac{1 - \exp(-\lambda t_1)}{\lambda t_1} \exp(-\lambda t_2) . \quad (3)$$

The first factor takes into account the probes directly produced as ^{111}In by nuclear reactions. f_{EC} denotes the fraction of ^{111}Sn atoms which decay to the ground state of ^{111}In via EC. The third factor considers the ^{111}Sn nuclei that decay during irradiation, while the fourth factor describes the radioactive decay of ^{111}Sn between end of irradiation and time zero. λ is the decay constant of ^{111}Sn and is given by $\lambda = \ln 2 / 35 \text{ min} = 1/50 \text{ min}$. By means of Eq. (3) we obtain $f_n = 0.35 \pm 0.04$.

C. PAC and data analysis

The PAC is measured for the 171–245-keV γ cascade of ^{111}Cd following the decay of ^{111}In .²⁰ Thus, the interaction of the $5/2^+$ isomeric nuclear state of ^{111}Cd ($T_{1/2} = 85 \text{ ns}$) with an extranuclear electric-field-gradient (EFG) tensor can be observed. For polycrystalline samples the strength (eq) and symmetry (η) of the EFG tensor can be determined. Usually the quadrupole coupling constant $\nu_Q = e^2qQ/h$ (where Q is the probe's nuclear electric quadrupole moment) and the dimensionless parameter η are given. If a certain fraction f_1 of the probes is decorated with a uniform defect with $\eta = 0$ (axial symmetry), while the remaining fraction $(1 - f_1)$ is located on sites with cubic symmetry, the PAC spectrum, $R(t)$, takes the following form:⁷

$$\begin{aligned} R(t) &= (1 - f_1) A_{22} + f_1 A_{22} G_{22}(t) \\ &= A_{22} \left[(1 - f_1) + f_1 \sum_{n=0}^3 s_{2n} \cos[(3\pi/10)n\nu_Q t] \right] . \end{aligned} \quad (4)$$

The anisotropy coefficient A_{22} is $A_{22} = -0.179$ in this case. The experimentally observed A_{22} is somewhat smaller mainly due to the finite solid angle of the γ counters. $G_{22}(t)$ is the time-dependent perturbation factor, which in the considered case is the sum of a constant and three cosines with the harmonic frequency ratio 1:2:3. The frequencies are weighted by the amplitudes s_{2n} , which are tabulated. For the fraction $(1 - f_1)$ no modulation is obtained since the EFG vanishes for a cubic lattice site.

In a conventional four-detector setup²¹ 12 delayed $\gamma\gamma$ -coincidence spectra $I_k(\theta, t)$ were recorded (with θ being the angle between two γ counters). After correcting the spectra for statistical background the experimental $R(t)$ spectrum was calculated as follows:

$$R(t) = \frac{2}{3} \left[\frac{\left[\prod_{k=1}^4 I_k(180^\circ, t) \right]^{1/4}}{\left[\prod_{k=1}^8 I_k(90^\circ, t) \right]^{1/8}} - 1 \right]. \quad (5)$$

By means of Fourier analysis the harmonic frequency ratio 1:2:3 was confirmed for all measured spectra. We,

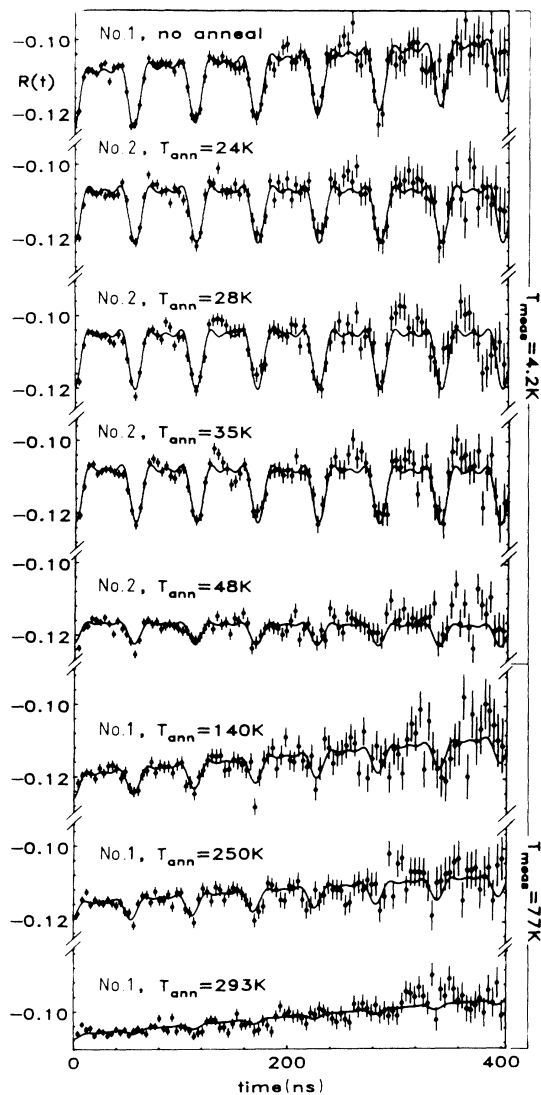


FIG. 1. PAC spectra of the measuring runs nos. 1 and 2. The neutrino emission in the electron capture decay $^{111}\text{Sn} \rightarrow ^{111}\text{In}$ leads to the production of single FP's at 4.2 K in otherwise undamaged copper. As a result the signal of the monovacancy on a nearest-neighbor site with respect to the ^{111}In - ^{111}Cd probe is observed ($\nu_Q = 117$ MHz, $\eta = 0$). The fate of these monovacancies is followed up in an isochronal (10 min) annealing program. The amplitude of the defect signal is described by the parameter f_1 which is plotted in Fig. 2.

therefore, used Eq. (4) for the least-squares fits to the time spectra with f_1 and ν_Q as the only free parameters. In Fig. 1 the spectra and the fitted curves (solid lines) are shown. All spectra yield the same $\nu_Q = (117 \pm 1)$ MHz. The fraction f_1 as a function of annealing temperature is plotted in Fig. 2.

Some spectra show slight deviations from the fitted curves. A very careful and detailed analysis including Fourier transforms shows, however, that it is not possible to improve the quality of the fit by introducing a second set of defect parameters (f_2, ν_{Q2}, η_2). We therefore conclude that these deviations are either due to small systematical errors or stem from various additional defect fractions f_2, f_3, \dots, f_n , which are no longer resolvable. In the latter case we estimate that the sum $f_2 + f_3 + \dots + f_n$ is smaller than 1%. Furthermore, the spectra of run no. 1 show a slight decrease of anisotropy as a function of time. This effect was considered by a Lorentzian frequency distribution around $\nu_Q = 0$. The fit yields a value of 0.32 ± 0.02 MHz for the full width at half maximum (FWHM) of this distribution. Since the samples of both measuring runs were treated identically except that the samples of run 1 were simply dropped into LHe, while those of run no. 2 were slowly lowered into LHe, we suspect that the rapid cooling down performed in run 1 is responsible for the effect. A comparison of the "no-annealing" spectra of both runs proves that the FP production is obviously not influenced by the different cooling rates.

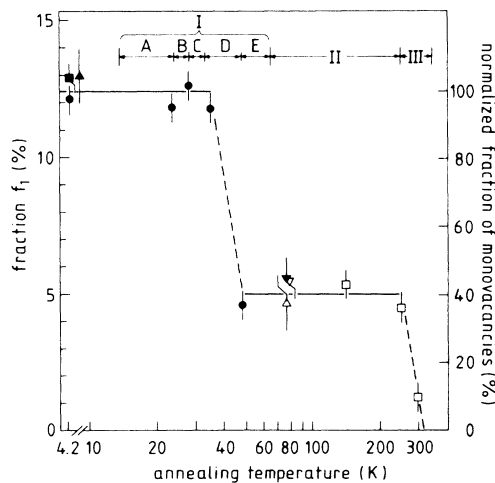


FIG. 2. The fraction f_1 of probes decorated with monovacancies as a function of annealing temperature. The solid lines represent weighted averages over the data points in the respective temperature regions. The low-temperature average of f_1 is used to normalize the fraction of monovacancy-probe pairs to 100%. About 60% of the monovacancies are annihilated by their own interstitial (correlated recombination) in the temperature region of stage I_D . The remaining monovacancies detrap and vanish in stage III. (The locations of the annealing stages are taken from Ref. 4.)

III. DISCUSSION

A. Assignment of the defect signal

Before we can discuss various aspects of FP production and annealing, we have to make an assignment for the observed defect-induced signal ($\nu_Q = 117$ MHz, $\eta = 0$). The check experiment with the ^{111}In probe⁸ shows that the signal stems from neutrino-recoil atoms which start from substitutional lattice sites. We know from the comparison of the minimum displacement threshold to the recoil energy of the probe that by each probe at most one FP can be produced. The extremely low probe concentration of 10^{-3} atomic ppm ensures that these FP's do not influence each other. Therefore, the signal is due to either a monovacancy or a monointerstitial. The signal cannot be caused by both defects simultaneously since there has to be a minimum distance between the Frenkel partners in order to escape spontaneous recombination. This distance together with the short-range nature of the quadrupole interaction ensure that the signal is essentially induced by the Frenkel partner which is closer to the probe. But even a small possible influence of the distant Frenkel partner is excluded since we find a clear uniform signal.

Furthermore, the same ν_Q of 117 MHz ($\eta = 0$) was observed by Wichert *et al.* in experiments in which the ^{111}In - ^{111}Cd probe was used as a trapping agent for point defects in copper.²² In these experiments the signal occurred after isochronal anneals in stage III as the result of a trapping process. We assume, of course, that the underlying defect is the same as in our experiment. This is confirmed by the fact that in both experiments detrapping of the 117-MHz defect occurs at 300 K (see also Sec. III C).

The question of which type of defect is really observed in our experiment can best be discussed by considering the possible scenarios for the neutrino-recoil effect (see also Ref. 8).

Scenario 1. Here we assume that the ^{111}In recoil atom leaves its lattice site and forms an interstitial configuration some distance away. The original lattice site of the probe will be left as a vacancy, which is, however, invisible in the PAC spectrum. In this scenario the 117-MHz signal is due to the monointerstitial.

Scenario 2. The ^{111}In recoil atom initiates a replacement collision sequence along a close-packed lattice direction. Such replacement collision sequences are possibly accompanied by focusing effects and lead to a monovacancy next to the PKA and a monointerstitial at a distance. Therefore, in this scenario the 117-MHz signal has to be assigned to the monovacancy.

In the following we show that a decision between both scenarios is possible. The argument is based on the observation of correlated recombination. Annealing of the samples to 48 K leads to a reduction of the defect signal of $\approx 60\%$, whereas it remained constant up to 35-K annealing temperature (see Fig. 1). This means that for $\approx 60\%$ of the probes that were originally decorated with the 117-MHz defect the cubic symmetry is restored by a thermally activated process in that temperature range. The low probe concentration combined with the fact

that the dissociation of the probe-defect pair does not occur below ≈ 300 K implies that only correlated recombination of FP's can account for this effect.

Moreover, from the thermal stability of the observed probe-defect pair we conclude that it is the invisible Frenkel partner which is thermally activated at ≈ 40 K and which may either recombine with the observed one or escape. Since only interstitial mobility comes into question at such low temperatures,⁴ the invisible Frenkel partner is the monointerstitial and the monovacancy is the observed one. Thus it is the monovacancy which causes the 117-MHz signal, and scenario 2 is the correct description of FP production here.

This reasoning is in perfect agreement with the classical work of Corbett, Smith, and Walker (CSW), who have shown that *free interstitial migration* leads to correlated recombination of FP's in stage I_D (between 33 and 48 K) of pure copper. The fact that correlated recombination in our experiment takes place in just that temperature interval supports the fact that the probes do not have a considerable influence on the correlated annihilation process but that the latter is an effect of the thermally activated migration of the monointerstitials.

The above assignment of the 117-MHz defect is fully independent of the interpretation of Wichert *et al.*, who, nevertheless, came to the same result.²² They conclude the vacancy character of the 117-MHz defect from its appearance after quenching. By way of comparing different irradiation experiments they then identify it as the *monovacancy*.

Deicher *et al.* observed PAC signals due to interstitial trapping at ^{111}In at the end of stage I in copper.²³ Those signals are completely different from the signal we observe so that their result yields another independent support that we definitely do not observe the defect mobile in $I_{D,E}$ but rather its antidefect.

B. Mechanism of Frenkel-pair production

We now discuss the correct scenario 2 of the foregoing section in some detail. It is essential for this discussion that in the present experiment the monovacancy-probe pair occurs in the same configuration as in the trapping experiments of Wichert *et al.*²² These authors also performed PAC experiments using copper single crystals and thus determined $\langle 110 \rangle$ as the symmetry axis of the EFG tensor of the 117-MHz defect.²⁴ (A PAC single-crystal experiment combined with the neutrino-recoil effect is hampered by serious experimental difficulties.) Therefore, in both experiments the monovacancy is located on a nearest-neighbor site relative to the ^{111}In - ^{111}Cd probe. However, there is an important difference between both experiments: Wichert *et al.* observed a thermally activated trapping process while we are confronted with an athermal recoil process. Therefore, the observed configuration does in our case contain information on the FP production process. This becomes evident when we turn to the monovacancy-PKA configurations that are expected for pure copper at low PKA energies.⁵ Two configurations, *A* and *B*, should occur.

Configuration A is the result of a replacement collision sequence along a $\langle 110 \rangle$ direction. This collision sequence is accompanied by Silsbee focusing and is also called “dynamic crowdion.” The $\langle 110 \rangle$ collision sequence is expected to lead to the most distant FP’s in the low-energy regime.⁵ The PKA comes to rest on a former nearest-neighbor site, while the original site of the PKA is left as a vacancy.¹¹ Obviously configuration *A* corresponds to the experimentally observed probe-monovacancy pair. This suggests that we also observe FP production via replacement collisions along $\langle 110 \rangle$.

Configuration B occurs as a result of a replacement collision sequence along a $\langle 100 \rangle$ direction. Atoms along this direction are too widely spaced for Silsbee focusing. A possible explanation for the fact that the threshold energy for $\langle 100 \rangle$ is as low as for $\langle 110 \rangle$ is based on the effect of assisted focusing which was found by computer simulation.⁵ Configuration *B* consists of a second-nearest-neighbor monovacancy with respect to the PKA (probe).

In our experiment this configuration would lead to an EFG with axial symmetry ($\eta=0$) around $\langle 100 \rangle$ and $\nu_Q \approx (1/\sqrt{2})^3(117 \text{ MHz}) \approx 41 \text{ MHz}$. The given estimate for ν_Q is based on the point-charge model. Due to screening effects the real value will very likely be even lower.²⁵ Obviously, configuration *B* is not observed in our experiment.

We discuss possible explanations for the fact that configuration *B* is missing, while *A* occurs. First one might argue that assisted focusing is an artifact of computer simulations. In fact, early measurements with polycrystalline copper could be explained by considering $\langle 110 \rangle$ replacement sequences only,²⁶ or either $\langle 100 \rangle$ or $\langle 110 \rangle$ replacement sequences only.²⁷ However, various experiments with single crystals show that both $\langle 100 \rangle$ and $\langle 110 \rangle$ directions exhibit the same low displacement threshold, indicating that both types of replacement sequences really occur in pure copper.¹

So if we postulate that the In impurity also produces FP’s via replacement collisions both along $\langle 110 \rangle$ and $\langle 100 \rangle$, we have to assume that configuration *B* is initially formed but relaxes into configuration *A* as an aftereffect of the recoil process. This appears to be quite plausible, since configuration *A*, in contrast to *B*, is also observed in trapping experiments,²² indicating its favorable energetic position.

Another explanation for the absence of configuration *B* is that no stable FP’s are formed by $\langle 100 \rangle$ replacement collision sequences due to the impurity character of the PKA (probe). The reason could be an increased threshold along $\langle 100 \rangle$. Thomson has shown that the threshold for FP production along $\langle 100 \rangle$ is mainly determined by the potential energy of the PKA within the window of four nearest neighbors which the PKA has to pass in order to hit a $\langle 100 \rangle$ neighbor.²⁸ This potential energy will be considerably increased—compared to a copper atom—for an oversized impurity like the In atom, so that the given recoil energy might be too low to produce a stable FP in that manner.

Thus our experiment alone does not allow us to decide which is the correct explanation for the absence of

configuration *B*. However, some preference for the latter explanation follows from the low probability P_{FP} of FP production by the ¹¹¹In PKA. P_{FP} is given by

$$P_{\text{FP}} = f_1(4.2 \text{ K})/f_n = 0.125(5)/0.35(4) = 0.36(4) .$$

$f_1(4.2 \text{ K})$ is the fraction of probes initially decorated with the monovacancy, while f_n denotes the fraction of probes that are capable of producing a FP (see Sec. II B). If we assume that the probe behaves like a copper PKA of 27 eV we would expect a P_{FP} value of 0.5 (Ref. 3) or even 1.0 (Ref. 2).

The measured lower value is consistent with $\langle 110 \rangle$ replacement collision chains as the only FP production mechanism (see Appendix). Moreover, replacement collision chains along $\langle 100 \rangle$ are assumed to lead to close FP’s.¹ The absence of this production process would therefore help to explain the total or nearly total absence of close-pair recovery which is discussed in the following section.

It would be very instructive to compare our experimental results concerning FP production to a computer simulation with an oversized PKA. To our knowledge no such calculations have yet been performed.²⁹

C. Frenkel-pair recovery

We now turn our attention to details of the annealing curve (Fig. 2). These are best discussed in connection with the classical work of Corbett, Smith, and Walker (CSW), who extensively investigated stage-I recovery of pure copper following electron irradiation.⁴ CSW determined five substages, I_{A-E} , of stage I and presented evidence for the following interpretation.

In the stages I_A , I_B , and I_C different types of close FP’s undergo correlated recombination. Close-pair recombination is assisted by elastic forces, and thus occurs at lower temperatures than free interstitial migration. The interstitial of a close pair cannot escape recombination. CSW found close-pair recovery for 25.6% of all produced FP’s. In stages I_D and I_E free interstitial migration takes place and leads, in stage I_D , to correlated and, in stage I_E , to uncorrelated recombination of FP’s.

As the PAC method does not allow us to measure annealing curves of an accuracy comparable to resistivity measurements (that were done by CSW), we let our annealing temperatures coincide with the upper temperature limits of the annealing stages of CSW. The intention was to find out whether similar annealing processes occurred in our experiment. The result is shown in Fig. 2. The straight lines represent weighted averages over the data points in the respective temperature regions, while the dashed lines only serve to guide the eye. It is apparent that both straight lines describe the data quite well, which means that the data are compatible with no change in f_1 , i.e., no FP recovery, in the respective temperature regions. For the right-hand scale of Fig. 2 the low-temperature average of f_1 was set to 100%. Using this scale, the experimental error of both plateaus is $\pm 4\%$, which means that the maximum recovery in the plateau regions is 8%. At the top of Fig. 2 the recovery

stages of CSW are indicated. Within the discussed limits of our experimental errors we can state the following. There is no recovery comparable to CSW in the close-pair region up to 35(2) K. Only in a stage of free interstitial migration, I_D , does approximately 60% of the FP's undergo correlated recombination. Also, there is no uncorrelated recombination in stage I_E , or a considerable recovery process in stage II. In stage III the remaining $\approx 40\%$ of the monovacancies detrapp and vanish via free migration. As mentioned before, the absence of uncorrelated recombination is readily explained by the low probe concentration of 10^{-3} atomic ppm, which yields a FP concentration of 10^{-4} atomic ppm. For the same reason a stage-II process in which, e.g., an interstitial is detrapped from another impurity and then recombines with an observed vacancy, is excluded.

The fact that there is no significant close-pair recovery, however, is at first glance somewhat surprising. As has already been mentioned briefly in the foregoing section, this is readily understood if no close pairs are produced by the ^{111}In PKA. In fact, we believe that this is the correct interpretation, although two objections can be raised.

First, one might think that the lower the PKA energy becomes the shorter the distance between the partners of the produced FP should be. Consequently, in our experiment, in which the effective PKA energy is only $\approx 40\%$ above the minimum threshold for displacement, preferentially close pairs should be produced. However, this simple view neglects peculiarities of FP production at low energies intimately connected with lattice structure and focusing effects.^{5,10}

Second, one might argue that the recovery process of close pairs is different from the one in pure copper due to a modified elastic interaction induced by the ^{111}In impurity. This could then lead to a temperature shift of close-pair stages either to higher or lower temperatures. In the latter case the data could be explained if one assumes that the close-pair stages are shifted to ≈ 4.2 K or below. This leads, of course, only to a semantic difference to our interpretation given above, namely, that no close pairs are produced at 4.2 K.

We now consider the possibility that close-pair stages are shifted to higher temperatures and accidentally coincide with stage I_D . This interpretation would require a rather complicated microscopic situation which we do not intend to speculate about. We rather show by a quantitative comparison with the data of CSW that close-pair recovery can largely be excluded for our experiment. The argument is based on the fractions of recovery given by CSW for the different stages, and the fact that close pairs undergo 100% recovery. We can calculate the fraction of correlated recombination, f_{CR} , from the relative numbers of close (f_{CP}) and distant (f_{DP}) FP's ($f_{\text{DP}} + f_{\text{CP}} = 100\%$):

$$f_{\text{CR}} = (100f_{\text{CP}} + 65.6f_{\text{DP}})\% . \quad (6)$$

The value of 65.6% is given by the recovery in I_D (48.8%) relative to 74.4%, which is the total (100%) minus close-pair recovery (25.6%). Therefore, the chance of an interstitial of a distant FP to find its own

vacancy in the experiment of CSW is 65.6%. Comparison with our value of $f_{\text{CR}} = 60(4)\%$ immediately yields $f_{\text{CP}} \approx 0\%$, which means that we observe no close-pair recovery. Otherwise, we would expect a larger amount of recovery at low temperatures.

An independent support for the above interpretation stems from the experiments of Lennartz *et al.*,³⁰ which also show that in pure Cu $\approx 60\%$ of those FP's that survived close-pair recovery undergo correlated recombination via free interstitial migration.

D. Consequences for defect models

In the preceding sections we have given an interpretation of our data without making use of specific features of the one-interstitial model³¹ or the two-interstitial model,³² which we shall henceforth call OIM and TIM, respectively. Since we only observe the monovacancy, we cannot decide in which configuration the copper monointerstitial occurs at low temperatures. However, this is the main difference of the conflicting models. In the TIM it is assumed that at low temperatures (stage $I_{D,E}$) only one form of the self-interstitial—the crowdion³³—is mobile. Crowdions may under certain conditions be converted into $\langle 100 \rangle$ dumbbells which only become mobile in stage III. According to this model vacancies get mobile only above stage III.

In the OIM the only stable form of the self-interstitial is the $\langle 100 \rangle$ dumbbell,³³ which is mobile in stage $I_{D,E}$. Stage III is interpreted in terms of vacancy migration.

Our experimental observations, namely, the recovery of part of the observed monovacancies induced by freely migrating interstitials in stage I_D and the detrapping of the remaining vacancies in stage III, are in perfect agreement with the OIM.

Nevertheless, based on the limited data of our previous publication,⁸ Frank has interpreted our experiment in terms of the TIM as follows.³⁴ The 117-MHz signal is induced by the monointerstitial, and the low-temperature recovery is of close-pair type. The elastic forces that act during this type of recovery explain, in Frank's opinion, that correlated recombination is already possible at very low temperatures although the monovacancy *alone* is immobile and the 117-MHz probe-defect pair *alone* is thermally stable up to 300 K. Frank's interpretation requires a very high binding energy of ≈ 0.7 eV between the interstitial and the oversized ^{111}In impurity. This cannot be explained by a hypothetical conversion of a crowdion into a dumbbell configuration, since the hyperfine parameters including the $\langle 110 \rangle$ symmetry axis of the observed probe-defect pair do not change irrespective of different measuring (4.2 or 77 K) or annealing temperatures. It must furthermore be assumed that this strong bond is easily broken by a monovacancy located out of the spontaneous recombination volume, i.e., outside the region of strong elastic interaction.

In light of the new recovery data presented in this paper, three assumptions or predictions, respectively, made by Frank have turned out to be unfounded. First, we do

not find close-pair recovery as predicted by Frank, but rather correlated recombination via free interstitial migration. Second, the annealing curve (Fig. 2) does not show a recovery *spectrum* up to 300 K as expected by Frank, but rather two well-defined stages fully consistent with the OIM. Third, the thermal stability of the probe-defect pair (117 MHz) is not altered by the unobserved Frenkel partner, since the detrapping occurs at the same temperature (300 K) as in the experiments of Wichert *et al.*²² In the framework of our interpretation the latter is not surprising since the monointerstials *all* vanish in stage $I_{D,E}$ and thus do not affect the probes (decorated or not with the monovacancy) at higher temperatures.

In Frank's picture, the monovacancy as the antidefect of the observed one is present at all annealing temperatures. Therefore the question arises, why part of the monovacancies should so strongly act on the assumed probe-interstitial pair without, however, affecting the sensitive hyperfine parameters, while for the remaining FP's the monovacancy acts as if being absent.

Frank also argued that the fraction of 117-MHz defects that survived stage-I recovery was too large from the viewpoint of the OIM, which he thus excludes. We have already shown (see Sec. III C) that this argument is not valid in the absence of close pairs.

Another important point makes it difficult to believe that our experimental findings can be brought into accord with the TIM. Our experiment yields clear evidence for dynamic crowdions, i.e., focused replacement collision sequences along $\langle 110 \rangle$. Thus (meta)stable crowdions, as they are postulated by the TIM, can, *a priori*, not be excluded. However, a replacement collision sequence leads to an interstitial formed at the *end* of the sequence. The interstitial can therefore not include the PKA. On the other hand, if the 117-MHz signal was induced by the monointerstitial, this interstitial-probe complex would have to be present in a crowdion-like configuration due to the $\langle 110 \rangle$ symmetry of this defect. Since the probe *is* the PKA, this leads to a contradiction in terms for the TIM: To save the concept of the (meta)stable crowdion, the concept of the dynamic crowdion, which is required for the production of the (meta)stable one,²⁷ has to be given up.

IV. CONCLUSIONS

We have shown that ^{111}In neutrino-recoil atoms can be used to create isolated single FP's in copper. Thus FP production and annealing could be investigated on an atomic scale. In detail, the following self-consistent interpretation was obtained. The FP's are produced via focused replacement collision sequences along $\langle 110 \rangle$. This production process leads to rather distant FP's and a monovacancy being the nearest neighbor of the ^{111}In PKA (117-MHz signal). The monointerstials are produced at a distance so that they do not affect the ^{111}In - ^{111}Cd PAC. The relatively low FP production probability of 0.36(4), and the fact that no probe-vacancy pairs with $\langle 100 \rangle$ symmetry axis appear, suggest that $\langle 100 \rangle$ replacement collision sequences (possibly accompanied

by assisted focusing) are hampered for the oversized PKA, the ^{111}In probe. This concurs with the fact that we find no significant close-pair recovery (for which our experiment yields 8% of the total FP recovery as an upper limit), since $\langle 100 \rangle$ replacement collision sequences are believed to lead to close FP's.¹ In stage I_D correlated FP recombination via free interstitial migration takes place and leads to a recovery of $\approx 60\%$ of the initially observed monovacancies. This amount of recovery is in good agreement with data for pure copper^{4,30} if again a more or less total absence of close pairs is assumed. In stage III the remaining monovacancies detrapp from the probes and disappear via free migration.

The experimental findings confirm the interpretation of trapping experiments with ^{111}In - $^{111}\text{CdCu}$.²² All details of the FP recovery process are in perfect agreement with the one-interstitial model. An attempt to interpret the data in terms of the two-interstitial model³⁴ leads to serious inconsistencies.

APPENDIX: EFFECT OF AN OVERSIZED PKA ON SILSBEE FOCUSING

In a collision sequence in a straight chain of equally spaced hard spheres of equal mass and radius, the angle at which the spheres leave the chain axis may either increase (defocusing) or decrease (focusing) in successive collisions. The focusing condition is $D/R < 2$ with spacing between centers of spheres, D , and sphere diameter R . If the focusing condition is fulfilled, focusing occurs, if the first sphere leaves the chain axis at an angle β_0 smaller than β_{\max} with $\beta_{\max} = \arccos(D/2R)$. The following equation (A1) describes how the kinetic energy E_{n+1} transferred from the n th sphere (with kinetic energy E_n) to the $(n+1)$ th sphere depends on the focusing parameter D/R and the starting angle β_n :³⁵

$$E_{n+1} = E_n [1 - (D/R)^2 \sin^2 \beta_n] . \quad (\text{A1})$$

One easily sees that the energy transfer increases for decreasing β_n and decreasing D/R . Since in our experiment the ^{111}In impurity plays the part of the PKA, we need only consider the first collision event and compare it to one in pure copper. For the latter case we can readily apply Eq. (A1):

$$E_1 = E_0 [1 - (D_{\text{Cu}}/R_{\text{Cu}})^2 \sin^2 \beta_0] . \quad (\text{A2})$$

$D_{\text{Cu}} = 2.55 \text{ \AA}$ is the nearest-neighbor distance in copper and R_{Cu} is the hard-sphere diameter of a copper atom. R_{Cu} which is energy dependent can be calculated from a two-body potential $V(r)$ by the condition $V(R_{\text{Cu}}) = E_0/2$.¹⁰ For the potential used by Gibson *et al.*⁵ and $E_0 = 30 \text{ eV}$, we get $R_{\text{Cu}} = 1.44 \text{ \AA}$ and thus $D_{\text{Cu}}/R_{\text{Cu}} = 1.77$, i.e., focusing. For the case of the ^{111}In atom acting as PKA, Eq. (A1) has to be modified as follows:

$$E_1 = 4m_{\text{Cu}}m_{\text{In}}(m_{\text{Cu}} + m_{\text{In}})^{-2} \times E_0 \{1 - [2D_{\text{Cu}}/(R_{\text{In}} + R_{\text{Cu}})]^2 \sin^2 \beta_0\} . \quad (\text{A3})$$

The first term considers the different masses of copper and indium atoms and has a value of 0.93. For the modified focusing parameter we assume that the lattice spacing D_{Cu} is not affected by the impurity. For R_{In} we insert $R_{\text{In}} = 1.21R_{\text{Cu}}$, a value taken from the table of King.¹⁷ The focusing parameter is now 1.60, i.e., focusing is improved. The reason why the angle dependence can be retained from Eq. (A1) is that in hard-sphere collisions the recoil angle of the target sphere is independent of the mass ratio of the colliding spheres.³⁶ Equations (A2) and (A3) can now be used to calculate the relative energy transfer E_1/E_0 in the first collision as a function of starting angle β_0 . In Figure 3 we have plotted the result. For $\beta_0 < 16^\circ$ the first collision is more effective in pure copper (solid line) because of the equal masses. For $\beta_0 > 16^\circ$ the In PKA (dashed line) transfers more energy, since the positive effect of the larger atomic radius then dominates. The latter effect is also responsible for the higher value of β_{max} , the starting angle up to which focusing occurs. While for pure copper β_{max} is 28° , $\beta'_{\text{max}} = 37^\circ$ for the impurity case is obtained. It is apparent from Fig. 3 that if all first collisions with β_0 smaller than β_{max} or β'_{max} , respectively, finally led to the production of a stable Frenkel pair, an In PKA would be more efficient in FP production than a Cu PKA of the same starting energy E_0 . However, in our experiment E_0 has the fixed value of $E_0 = 29$ eV, a value too low to allow for FP production at high starting angles. This becomes evident if one looks at the right-hand scale of Fig. 3, where the absolute values of E_1 are given for $E_0 = 29$ eV. It is reasonable to assume that a stable FP is produced only if E_1 lies above or close to the threshold of 19 eV. This is only true for starting angles below $\approx 20^\circ$, a region where the better focusing characteristics of the In PKA are of no importance.

From the above considerations in the hard-spheres approximation we can therefore conclude that the In PKA should largely behave the same as a Cu PKA of comparable kinetic energy, and that both PKA's will produce FP's via Silsbee focusing with about the same probability.

It is interesting to note that the condition $\beta_0 \leq 20^\circ$

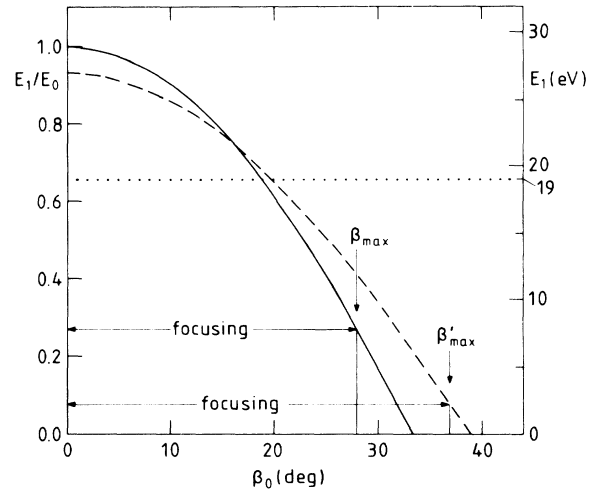


FIG. 3. Relative amount of energy transferred in a Cu-on-Cu (solid line) and a In-on-Cu (dashed line) collision as a function of starting angle β_0 in the hard-spheres approximation. The oversized In atom cannot transfer all its kinetic energy to a Cu neighbor, but it shows better focusing characteristics. The (absolute) energy scale on the right-hand side refers to the present experiment ($E_0 = 29$ eV). 19 eV is the minimum threshold energy for FP production in copper.

which corresponds to an energy transfer of more than 19 eV in the first collision leads to a probability of FP production of $P_{\text{FP}} = 0.36$. This value agrees amazingly well with the experimental P_{FP} of 0.36(4) (see Sec. III B). Therefore, $\langle 110 \rangle$ collision chains combined with Silsbee focusing can indeed account for *all* observed FP's.

ACKNOWLEDGMENTS

We thank Dorothea Alber for computing the reaction cross sections (see Sec. II B) and Bernd Spellmeyer for reading the manuscript critically. The financial support of the Deutsche Forschungsgemeinschaft (Sonderforschungsbereich 161) is gratefully acknowledged.

¹For a review, see P. Vajda, Rev. Mod. Phys. **49**, 481 (1977).

²P. Jung, R. L. Chaplin, H. J. Fenzl, K. Reichelt, and P. Wombacher, Phys. Rev. B **8**, 553 (1973).

³W. E. King, K. L. Merkle, and M. Meshii, J. Nucl. Mater. **117**, 12 (1983).

⁴J. W. Corbett, R. B. Smith, and R. M. Walker, Phys. Rev. **114**, 1452 (1959); **114**, 1460 (1959).

⁵J. B. Gibson, A. N. Goland, M. Milgram, and G. H. Vineyard, Phys. Rev. **120**, 1229 (1960).

⁶A. Tenenbaum, Philos. Mag. A **37**, 731 (1978).

⁷For a review, see E. Recknagel, G. Schatz, and Th. Wichert in *Hyperfine Interactions of Radioactive Nuclei*, edited by J. Christiansen (Springer, Heidelberg, 1983), p. 133.

⁸H. Metzner, R. Sielemann, R. Butt, and S. Klaumünzer, Phys. Rev. Lett. **53**, 290 (1984).

⁹A somewhat similar experiment was already performed in 1977 by Butt *et al.*, who used a γ -recoil process in combination with ^{111}Cd PAC in palladium. The recoil energy, however, was in this experiment too high to exclude multiple-defect production. R. Butt, H. Haas, T. Butz, W. Mansel, and A. Vasquez, Phys. Lett. **64A**, 309 (1977).

¹⁰R. H. Silsbee, J. Appl. Phys. **28**, 1246 (1957).

¹¹Computer simulations indicate that the PKA often returns to its original lattice site and the site of the second atom in the replacement sequence is left vacant. This could be different in the present experiment since the heavy ^{111}In PKA keeps part of its initial momentum even in a head-on collision.

¹²B. Harmatz, Nucl. Data Sheets **27**, 453 (1979).

¹³A direct consequence of the EC decay is a hole in the K shell of the ^{111}In atom. An electron from an outer shell will very

- quickly refill this vacant electronic state. This process is followed by the emission of Roentgen quanta and Auger electrons. The ^{111}In ion will reach a stable charge state in less than 10^{-14} s. This time has to be compared to the time of 3.5×10^{-14} s required by the ^{111}In ion of 29 eV to reach a neighboring lattice site in copper. Since the latter is considerably longer, we do not expect an influence of the electronic decay aftereffect on FP production. For details of decay aftereffects see, e.g., H. J. Leisi, *Phys. Rev. A* **1**, 1662 (1970).
- ¹⁴A. H. Wapstra and K. Bos, *At. Data Nucl. Data Tables* **19**, 177 (1977).
- ¹⁵Single-crystal samples and very low electron energies down to 500 keV have been used to try to overcome this problem. The results, however, are contradictory in some respects (see Ref. 1).
- ¹⁶O. S. Oen, Oak Ridge National Laboratory Report No. ORNL 4897, 1973 (unpublished).
- ¹⁷H. W. King, *J. Mater. Sci.* **1**, 79 (1966).
- ¹⁸H. Pühlhofer, *Nucl. Phys.* **A280**, 267 (1977).
- ¹⁹C. M. Lederer and V. S. Shirley, *Table of Isotopes*, 7th ed. (Wiley, New York, 1978).
- ²⁰The decay $^{111}\text{In} \xrightarrow{\text{EC}} ^{111}\text{Cd}$ leads to a recoil energy of 0.9 eV for the ^{111}Cd nucleus. This energy is by far too low for FP production in copper.
- ²¹H. Haas and D. A. Shirley, *J. Chem. Phys.* **58**, 3339 (1973).
- ²²Th. Wichert, M. Deicher, O. Echt, and E. Recknagel, *Phys. Rev. Lett.* **41**, 1659 (1978).
- ²³A comprehensive survey of the trapping experiments with the ^{111}In - ^{111}Cd probe in copper is given in M. Deicher, G. Grübel, R. Minde, E. Recknagel, and Th. Wichert, in *Yamada Conference V on Point Defects and Defect Interactions in Metals*, edited by J. Takamura, M. Doyama, and M. Kiritani (University of Tokyo Press, Tokyo, 1982), p. 220. The authors report trapping of interstitials in two configurations ($\nu_Q = 47$ MHz, $\eta = 0$ and $\nu_Q = 19$ MHz, $\eta = 1$) at the end of stage I.
- ²⁴M. Deicher, O. Echt, E. Recknagel, and Th. Wichert, in *Nuclear and Electron Resonance Spectroscopies Applied to Materials Science*, edited by E. Kaufmann and G. K. Shenoy (Elsevier/North-Holland, Amsterdam, 1981), p. 435.
- ²⁵It cannot be utterly excluded that the discussed configuration *B* is totally invisible, i.e., $\nu_Q \simeq 0$ MHz. This possibility is discussed by Müller for ^{111}In in a cubic alloy. H. G. Müller and H. Hahn, *Philos. Mag. A* **50**, 71 (1984).
- ²⁶A. Sosin, *Phys. Rev.* **126**, 1698 (1962).
- ²⁷R. V. Jan and A. Seeger, *Phys. Status Solidi* **3**, 465 (1963).
- ²⁸M. W. Thomson, *Defects and Radiation Damage in Metals* (Cambridge University Press, Cambridge, 1969).
- ²⁹In a conference contribution by G. H. Vineyard computer calculations for a Cu₃Au alloy are mentioned. Focusing chains along $\langle 110 \rangle$ are also found for this alloy. It is, however, not mentioned whether $\langle 100 \rangle$ replacement chains do or do not occur. G. H. Vineyard, *J. Phys. Soc. Jpn.* **18**, Suppl. III, 144 (1963).
- ³⁰R. Lennartz, F. Dworschak, and H. Wollenberger, *J. Phys. F Met. Phys.* **7**, 2011 (1977).
- ³¹W. Schilling, P. Erhart, and K. Sonnenberg, in *Proceedings of an International Conference on Fundamental Aspects of Radiation Damage in Metals, Gatlinburg, Tennessee, 1975*, edited by Mark T. Robinson and F. W. Young, Jr. (National Technical Information Service, Springfield, Va., 1975), p. 470.
- ³²A. Seeger, *Proceedings of an International Conference on Fundamental Aspects of Radiation Damage in Metals, Gatlinburg, Tennessee, 1975*, Ref. 31, p. 493.
- ³³For a description and discussion of the various configurations of the single self-interstitial in copper, see R. A. Johnson and E. Brown, *Phys. Rev.* **127**, 446 (1962). Note that crowdion denotes the $\langle 110 \rangle$ split interstitial and that $\langle 100 \rangle$ dumbbell stands for the $\langle 100 \rangle$ split interstitial.
- ³⁴W. Frank, *Radiat. Eff. Lett.* **87**, 1 (1985).
- ³⁵Chr. Lehmann, in *Interaction of Radiation with Solids and Elementary Defect Production* (North-Holland, Amsterdam, 1977), p. 200.
- ³⁶The recoil angle θ_2 of the target sphere in the laboratory frame is given by $\theta_2 = \beta_0 + \beta_1$ in the considered case.